HADRON PHYSICS IN BABAR

G.D.Lafferty [a]
Department of Physics and Astronomy, The University of Manchester, Manchester M13 9PL, UK

*Abstract.*Some recent results in hadron physics from the BaBar experiment are discussed. In particular, the observation of two new charmed states, the $D_{sJ}^{*+}(2317)$ and the $D_{sJ}^{*+}(2457)$, is described, and results are presented on the first measurement of the rare decay mode of the B meson, $B^0 \to \pi^0\pi^0$.

1 The BaBar Experiment

The BaBar detector [1] is a general purpose, solenoidal, magnetic spectrometer at the PEP-II asymmetric-energy e^+e^- storage rings at the Stanford Linear Accelerator Center. Since 1999 the detector has been taking data at centre-of-mass energies on, and just below, the peak of the $\Upsilon(4S)$ resonance, colliding 9 GeV electrons with 3.1 GeV positrons. The main purpose of the experiment is to measure CP-violation in the B-meson system. However the e^+e^- collisions are also a copious source of light-flavour and charm $q\overline{q}$ pairs and also of τ-lepton pairs. This allows for a rich and varied programme of hadron physics in the experiment.

Up until 2002, BaBar had accumulated some 91 fb^{-1} of e^+e^- collision data, recorded both on and off the $\Upsilon(4S)$ resonance. During 2003, a further 35 fb^{-1} was added to the sample. With annihilation cross sections of about 1.3 nb for up-type quark pairs, 0.3 nb for down-type quarks and 0.9 nb for tau-pairs, there are correspondingly large data sets. In this short paper, I discuss two particular recent BaBar analyses, one topic from charm spectroscopy and one from rare hadronic B-meson decays.

The BaBar detector combines a precision silicon vertex-tracker with a drift chamber, both having dE/dx capability, a Cherenkov radiation detector (the DIRC), a caesium iodide electromagnetic calorimer and an iron flux-return system, for the 1.5 T solenoidal magnetic field, instrumented as a muon detector. BaBar thus has precision vertexing and tracking capability together with excellent particle identification for all species of stable particles, including K_s^0, and for $\pi^0 s$.

2 Charmed meson spectroscopy: the new D_{sJ} states

One of the most remarkable of recent results in particle physics has been BaBar's discovery of a new charmed, strange meson, the $D_{sJ}^*(2317)^+$ [2]. While most new particles start life as dubious, two or three standard-deviation bumps

[a] Presented at the 11th Lomonosov Conference on Elementary Particle Physics, Moscow, August 2003

on mass spectra (for example, the proposed pentaquark states that came to light at about the same time as the D_{sJ}), the $D^*_{sJ}(2317)^+$ was first seen as a dramatic peak of many standard deviations. Indeed, it is an interesting question as to why it escaped detection for so long. There is a lesson for us all to expect the unexpected.

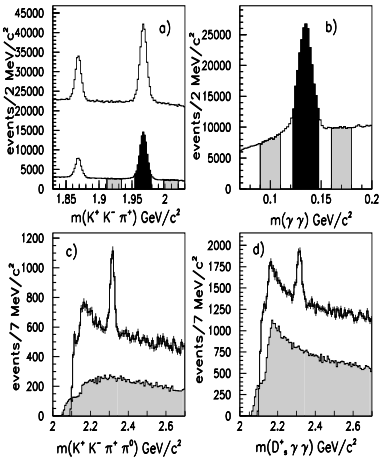

Figure 1: (a) The distribution of $K^+K^-\pi^+$ mass for all candidate events. Additional selection criteria have been used for the lower histogram. (b) The two-photon mass distribution from $D_s^+\pi^0$ candidate events. The D_s^+ and π^0 signal and sideband regions are shaded. (c) The $D_s^+\pi^0$ mass for candidates in the D_s^+ signal (top histogram) and $K^+K^-\pi^+$ sideband regions (shaded histogram) of (a). (d) The $D_s^+\gamma\gamma$ mass for signal D_s^+ candidates and a photon pair from the π^0 signal region of (b) (top histogram) and the sidebands region of (b) (shaded histogram).

The BaBar analysis used 91 fb^{-1} of data to investigate the inclusively-produced $D_s^+\pi^0$ mass spectrum. The technique was to combine charged particles from the decay $D_s^+ \to K^+K^-\pi^+$, measured in the tracking detectors, with π^0 candidates reconstructed from pairs of photons detected in the electromagnetic calorimeter. The kaon candidates were identified based on their Cherenkov radiation and their specific energy loss. Various cuts were applied to ensure a clean sample on a low background. The upper histogram in figure 1(a) shows the mass spectrum of the selected $K^+K^-\pi^+$ combinations. The two peaks are from the D^+ and D_s^+ mesons. The lower histogram of figure 1(a) shows the effect of selecting for the $\phi(1020)$ in K^+K^- or the $K^*(892)$ in $K^-\pi^+$. This plot shows the D_s^+ peak and sideband regions used in the subsequent analysis.

Figure 1(b) shows the spectrum of $\gamma\gamma$ pairs associated with the selected events, with peak and sideband regions indicated. Signal D_s^+ candidates are

combined with π^0 candidates to give the spectrum of figure 1(c). The shaded part shows the spectrum when π^0 candidates are combined with sideband entries in the $K^+K^-\pi^+$ mass spectrum. The dramatic peak near 2.32 GeV/c^2 is the new state, the $D^*_{sJ}(2317)^+$. Figure 1(d) shows the result of combining the D_s^+ candidates with the π^0 signal (unshaded) and sideband (shaded) regions.

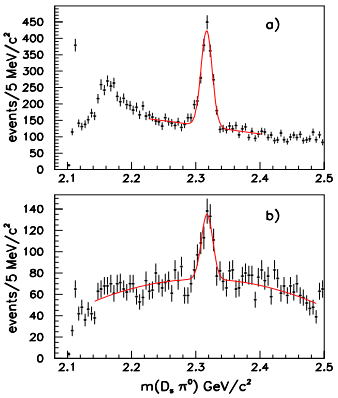

Figure 2: The $D_s^+\pi^0$ mass for (a) the decay $D_s^+ \to K^+K^-\pi^+$ and (b) the decay $D_s^+ \to K^+K^-\pi^+\pi^0$. The curves are from fits described in the text.

Figure 2 shows the mass spectrum of $D_s^+\pi^0$ candidates for two different D_s^+ decay modes and for some restricted kinematic ranges. The curves show fits using Gaussian functions, plus polynomials to describe the background. Consistent results are obtained from the two D_s^+ decay modes for the mass and the Gaussian width of the new peak. The fit in figure 2(a) yields a mass of 2316.8 ± 0.4 MeV/c^2 and a Gaussian width of $\sigma = 8.6 \pm 0.4$ MeV/c^2. Analysis of subchannels shows that this $D^*_{sJ}(2317)^+$ state is, as expected, seen in both the $\phi\pi^+$ and $\overline{K}^{*0}K^+$ decay modes of the D_s^+. The fitted Gaussian width is consistent with the mass resolution, so the intrinsic width of the $D^*_{sJ}(2317)$ is small, with $\Gamma < 10$ MeV/c^2.

Monte Carlo simulations have been used to verify that the 2.32 GeV/c^2 peak cannot be due to a reflection from some other charm state, nor from pion/kaon misidentification. The decay angular distribution is consistent with being flat, as expected for a spin-0 particle or for an unpolarized particle of any spin.

No evidence for other decay modes of the $D^*_{sJ}(2317)^+$ has been found. Figure 3 shows, for example, $D_s^+\gamma$, $D_s^+\gamma\gamma$ and $D_s^+\pi^0\gamma$ mass spectra for a number of cuts and selections, as described in the figure caption. While peaks are seen for $D_s^*(2112)^+$ and another apparent new state near 2.46 GeV/c^2, there is no

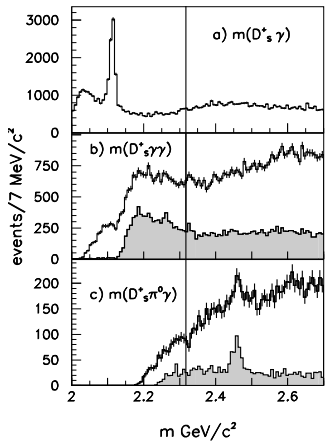

Figure 3: The mass distribution for (a) $D_s^+\gamma$ and (b) $D_s^+\gamma\gamma$ after excluding photons from the signal region of figure 1(b). (c) The $D_s^+\pi^0\gamma$ mass distribution. The lower histograms of (b) and (c) correspond to $D_s^+\gamma$ masses that fall in the $D_s^*(2112)^+$ signal region. The vertical line indicates the $D_{sJ}^*(2317)^+$ mass.

indication in any of these channels for the $D_{sJ}^*(2317)^+$.

At the time of publication of the discovery of the $D_{sJ}^*(2317)^+$ by BaBar, there was some uncertainty as to the nature of the second new peak at 2.46 GeV/c^2. The complexity of the overlapping kinematics of the $D_s^*(2112)^+ \to D_s^+\gamma$ and $D_{sJ}^*(2317)^+ \to D_s^+\pi^0$ decays needed further study to rule out the possibility of a kinematic artefact in $D_s^+\pi^0\gamma$ near 2.46 GeV/c^2. Subsequent work by Belle [3], CLEO [4] and BaBar [5] has confirmed the $D_{sJ}^*(2458)^+$ as a second, new charm state.

To investigate the $D_s^+\pi^0\gamma$ spectrum, D_s^+ candidates decaying to $K^-K^+\pi^+$ were used, from $c\bar{c}$ events recorded at centre-of-mass energy near 10.6 GeV, as described above. These candidates were combined with π^0 and γ candidates, as described in [5]. Figure 4(a) shows the resulting mass distribution, with a clear peak at 2.4 GeV/c^2. The background under the peak comes from several sources, which can be described in terms of mass differences: $\Delta m_\gamma = m(D_s^+\gamma) - m(D_s^+)$ and $\Delta m_{\pi^0} = m(D_s^+\gamma\pi^0) - m(D_s^+\gamma)$. The distributions of these are shown in the scatter plot of figure 4(b), indicating some kinematic effects that could possibly conspire to produce the peak at 2.4 GeV/c^2. The upper distribution of 4(c) shows $D_s^+\gamma\pi^0$ combinations corresponding to the $D_s^*(2112)^+$ signal region, and the shaded region to the corresponding sidebands. A fit to the subtracted distribution in figure 4(d) gives a narrow signal at $\Delta m_{\pi^0} = 346.2 \pm 0.9$ MeV/c^2.

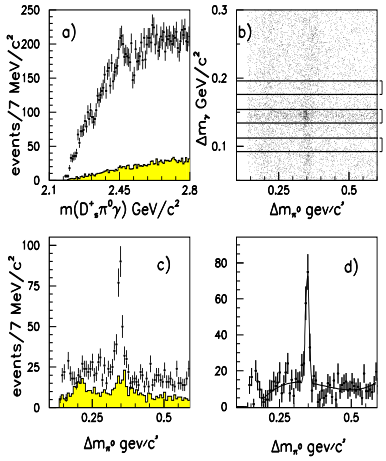

Figure 4: (a) The mass distribution for all selected $D_s^+\pi^0\gamma$ combinations. The shaded region is from D_s^+ sidebands ($1.912 < m(K^+K^-\pi^+) < 1.933$ GeV/c^2). (b) The value of Δm_γ versus Δm_{π^0} for all combinations. The horizontal lines indicate three ranges of Δm_γ. (c) The Δm_{π^0} mass distribution for the middle range of of Δm_γ (points) and for the average of the upper and lower ranges (shaded histogram). (d) The difference between the two distributions shown in (c). The curve shows the fit described in the text.

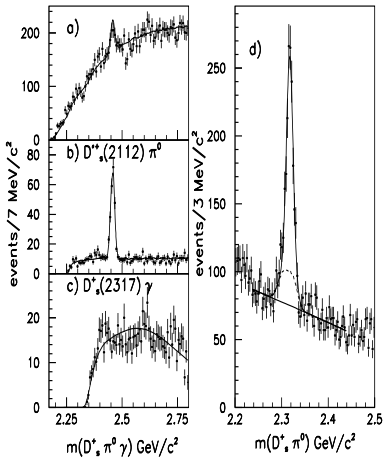

Figure 5: Maximum likelihood fit results overlaid on the $D_s^+\pi^0\gamma$ mass with (a) no weights, and after applying weights for (b) $D_s^*(2112)^+\pi^0$ and (c) $D_{sJ}^*(2317)^+\gamma$. (d) The mass spectrum of $D_s^+\pi^0$ (with no γ requirement). The solid curve is the fit described in detail in [5]. The dashed and lower solid curves are the contributions from $D_{sJ}^*(2458)^+$ decays and combinatorial background.

An unbinned maximum likelihood fit was used to disentangle the possible decay modes of the new state, the $D_{sJ}^*(2458)^+$, and to obtain reliable measures of the signal parameters. Full details of the fit are given in [5], and some results are shown in figure 5. The caption to the figure describes the distributions and the curves.

The measured mass of the $D_{sJ}^*(2458)^+$ is 2458.0 ± 1.4 MeV/c^2 which agrees with the Belle result [3], but is two standard deviations lower than that obtained by CLEO [4]. The measured width of the state is consistent with the experimental resolution. The yield relative to that of the $D_{sJ}^*(2317)^+$ also agrees with Belle, but is smaller than the yield reported by CLEO.

3 Rare B-meson decays

Determination of the angle α of the Unitarity Triangle using $B \to \pi\pi$ decays requires the use of isospin relations [6] between the amplitudes for the decays $B^0(\overline{B^0}) \to \pi^+\pi^-$, $B^0(\overline{B^0}) \to \pi^0\pi^0$ and $B^\pm \to \pi^\pm\pi^0$. The main contributions to the $\pi^0\pi^0$ channel come from colour-suppressed tree and gluonic penguin amplitudes, and the branching fraction has been calculated in a number of QCD models. For example, in a QCD factorisation model [7], the prediction is 0.3×10^{-6}. On the other hand, phenomenological fits to data on charmless B decays [8] give results in the range $(1.6 - 2.5) \times 10^{-6}$.

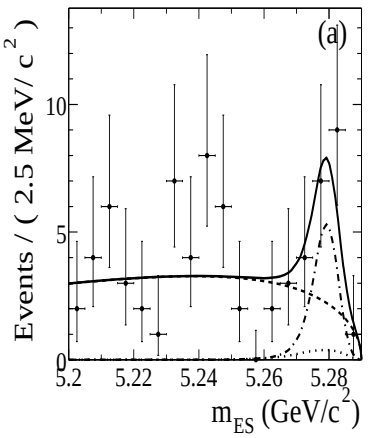

Figure 6: The distribution of $m_{\rm ES}$ for candidates in the $B \to \pi^0\pi^0$ signal data sample that satisfy an optimized requirement on the signal probability, based on all variables except $m_{\rm ES}$. The solid line shows the projection of the maximum-likelihood fit, with the dotted and dashed curves showing some non-signal contributions, as described in [9].

The BaBar study [9] used (124±1) million $\Upsilon(4S) \to B\overline{B}$ events, together with 12 fb^{-1} of data collected 40 MeV below the $\Upsilon(4S)$ peak. Candidate π^0 mesons were formed from selected photon pairs, reconstructed in the electromagnetic calorimeter, with invariant masses within 3σ of the π^0 mass, where the resolution σ is about 8 MeV/c^2 for high-momentum π^0 mesons. B-meson candidates were formed from combinations of two π^0 candidates. Two variables, used to isolate the $B \to \pi^0\pi^0$ signal, rely on the kinematic constraints for B meson pairs produced at the $\Upsilon(4S)$: these are the beam-energy-substituted mass, given by $m_{ES} = \sqrt{(s/2 + \mathbf{p}_i \cdot \mathbf{p}_B)^2/E_i^2 - \mathbf{p}_B^2}$, and the energy balance, given by $\Delta E = E_B - \sqrt{s}/2$. In these expressions, $\sqrt{s}$ is the total e^+e^- centre-of-mass energy, $(E_i, \mathbf{p}_i)$ is the four-momentum of the initial e^+e^- system in the lab frame, and $(E_B, \mathbf{p}_B)$ is the lab four-momentum of the B candidate. The ΔE resolution for signal is about 80 MeV.

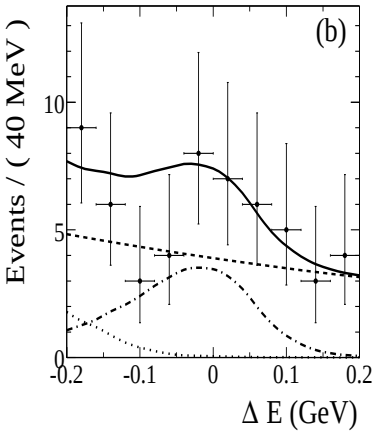

Figure 7: The distribution of ΔE for candidates in the $B \to \pi^0\pi^0$ signal data sample that satisfy an optimized requirement on the signal probability, based on all variables except ΔE. The solid line shows the projection of the maximum-likelihood fit, with the dotted and dashed curves showing some non-signal contributions, as described in [9].

Background sources of such pairs of π^0 mesons include $e^+e^- \to q\overline{q}$ events, where a π^0 from each quark jet can randomly combine to mimic a B decay. This background is suppressed using a cut on the angle between the sphericity axis of the B candidate and that of the rest of the tracks and photon candidates in the event. Background also comes from $B^\pm \to \rho^\pm\pi^0 \to \pi^\pm\pi^0\pi^0$ decays, in which the charged pion is emitted nearly at rest in the B rest frame.

An extended, unbinned maximum likelihood fit was used to measure the number of signal $B \to \pi^0\pi^0$ events, with, as inputs, the m_{ES} and ΔE variables

together with a Fisher discriminant, optimised to separate signal from background. The probability density functions for the fit were determined using both data and Monte Carlo simulation. Figures 6 and 7 show some projections of the fit. The fit gave a result of 46 ± 13 signal events in the sample, corresponding to a branching fraction $\mathrm{BR}(\mathrm{B} \to \pi^0\pi^0) = (2.1 \pm 0.6) \times 10^{-6}$. The significance of the signal was measured using the change in the likelihood value between the nominal fit and one with the signal yield fixed to zero. With statistical errors only, the significance is 4.7σ. An alternative event-counting analysis, with a lower efficiency, gave a consistent result. A large number of possible sources of systematic error were considered, leading to an expected systematic error of ± 3 signal events. This reduces the significance of the result to 4.2σ. The final branching ratio is then $\mathrm{BR}(\mathrm{B} \to \pi^0\pi^0) = (2.1 \pm 0.6 \pm 0.3) \times 10^{-6}$. This result is larger than some theoretical predictions, including those of the QCD factorisation model.

4 Conclusions

Hadron physics at BaBar is still at an early stage. In the first phases of the experiment, most attention was devoted to the physics of CP-violation. However the data sets contain copious amounts of $\mathrm{q\overline{q}}$ and $\tau^+\tau^-$ events, which will lead to an increasing, and varied, programme of hadron physics studies.

Acknowledgments

I would like to thank the committee of the 11th Lomonosov conference, and particularly Alexander Studenikin, for organising such a stimulating and interesting conference. I also thank the entire BaBar Collaboration and our PEP II colleagues; it is their work that is reported here.

References

[1] B. Aubert et al., BaBar Collaboration, *Nucl.Instr.Meth* A497, 1 (2002).
[2] B. Aubert et al., BaBar Collaboration, *Phys.Rev.Lett* 90, 242001 (2003).
[3] P. Krokovny et al., Belle Collaboration, submitted to *Phys.Rev.Lett* 92, 012002 (2004).
[4] D. Besson et al., CLEO Collaboration, *Phys.Rev.* D68, 032002 (2003).
[5] B. Aubert et al., BaBar Collaboration, *Phys.Rev.D* 69, 031101 2004.
[6] M. Gronau and D. London, *Phys.Rev.Lett* 65, 3381 (1990).
[7] See references [7] cited in [9].
[8] See references [8] cited in [9].
[9] B. Aubert et al., BaBar Collaboration, *Phys.Rev.Lett* 91, 241801 (2003).